Coulomb excitation experiment ^{58}Ni on ^{112}Sn at 175MeV

24.9.2008

Contents:

1. Kinematics

Calculations are performed with FORTRAN program: *kinemat.f*
(www-linux.gsi.de/~wolle/INDIA)

^{58}Ni projectile ($A_1=A_3=58$) on ^{112}Sn target nucleus ($A_2=A_4=112$) at E_{lab}=175MeV

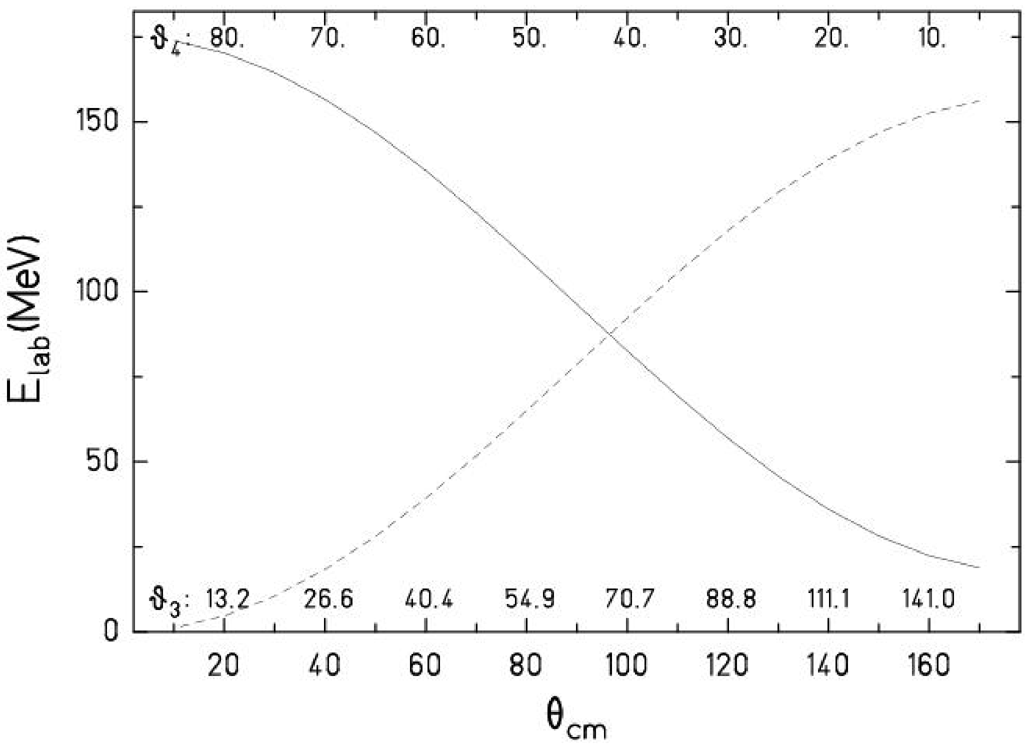

Fig. 1 shows the energy dependence of both reaction parameters on the scattering angle in the cm- and lab-frame.

The aim of the experiment is to measure either the projectile or the recoil nucleus in the annular PPAC (see fig.2). The PPAC can detect particles between 15^0 and 45^0. However, it can happen that particles at large scattering angles (at around ~45^0) are suppressed by the PPAC threshold because of their low energy. Therefore, it is doubtful, if the PPAC boundaries can be used for the calibration of the delay-line spectrum (see on-line analysis). An additional calibration point of the delay-line spectrum, which is proportional to $\tan(\vartheta)$, can be obtained from the scattering of the ^{58}Ni beam on an aluminium target. We will use the maximum kinematical angle (arc sin(27/58)=27.74^0) for the calibration. **I will carry a thin aluminium target (35µg/cm^2 and 90µg/cm^2) with me.**

2. Experimental setup

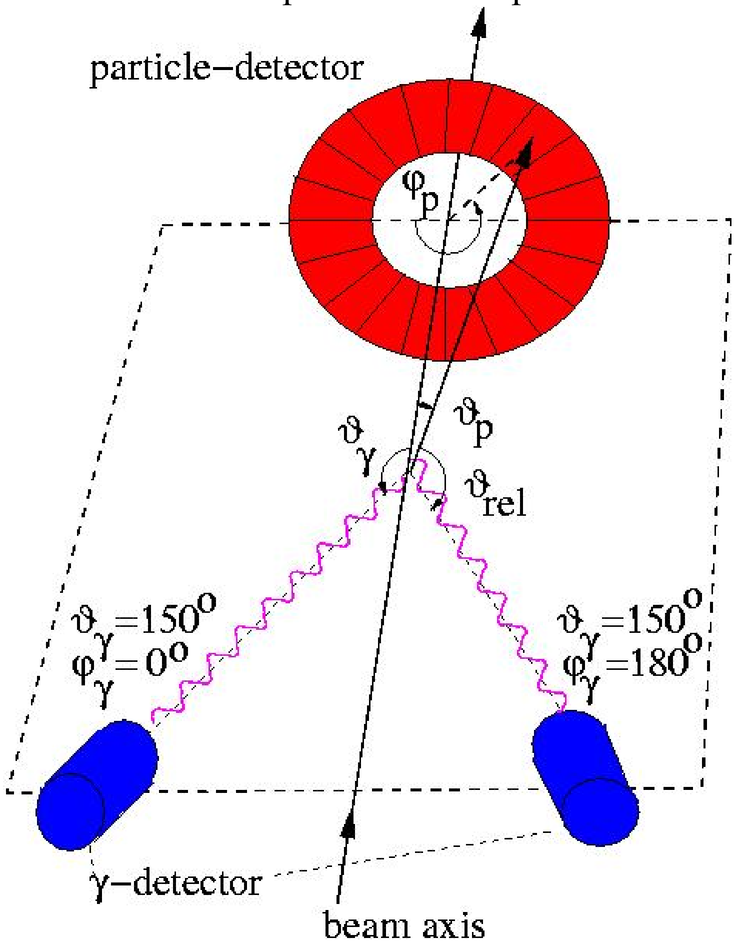

Fig.2 shows the experimental setup with the annular parallel plate avalanche counter (PPAC) and two Ge-detectors at backward angles.

The optimal setup will include four Clover Ge-detectors at backward angles (153^0). The azimuthal angles are 25^0, 155^0, 335^0 and 205^0. The front face radius of the Clover detector is r=3.25(6)cm. The intrinsic photopeak efficiency for the Clover detector is ε=0.20. The increase of the intrinsic photopeak efficiency from ε=0.13, the value for the individual Clover diodes, corresponds to the add-back factor.

Fig.3 shows the present GDA experimental setup.

Tasks:

Things to do for Coulomb Excitation experiment in GDA (Murali, 18-8-2008)

Check Vacuum in GDA beam line after mounting the Vent valve

Check the 200 lt dewar by LN2 filling from Main line while INGA / BH II 1000 lt periodic filling (alternate day)

Resurrect GDA LN2 auto fill system

Label existing GDA cable detector to Patch panel (PP), PP to electronics (inside GDA cabin)

Check inventory of modules & working condition

Mount plates with nylon / plastic screws

Mount ACS plates with 4 rods for clover to be mounted with it's own plate

Mobilize HVPS, PA-PS for clovers with necessary cables

Source testing with clover in GDA & CANDLE

convert CANDLE to Root for analyzing with GO4 / ROOT
cables / modules required (list given below)

Cable:
4 (Crystal) x 4 (Clover) x 2 (Energy / Time) = 32 signals to process in
Electronics cabin also
Detectors to Patch Panel Beam-line
Patch Panel to Clover modules
Clover modules to ADC, CO4010, GG8000, Mastergate

HV, Bias shutdown cables 4 each SHV to SHV (old & new are different) &
BNC to SBC / SMA

Preamplifier power cables

Electronics:
Bitpattern module testing
CF8000

Clover modules
GG8000
CO4010
4 8K quad ADC or equivalent
HVPS 5 KV, Preamplifier Power supply, preamplifier

1. The scattering chamber has to be mounted, aligned and vacuum tested.
2. The PPAC has to be attached downstream of the target (see fig.2) in order to measure scattering angles between 15^0 and 45^0.
3. The PPAC has to be tested with an alpha source (e.g. ^{241}Am).
4. 4 special plates for the INGA clovers have to be mounted.
5. 4 INGA clover detectors have to be positioned at backward angles (~150^0) and if possible at forward angles (~30^0).
6. All detectors have to be cabled.

3. Electronics

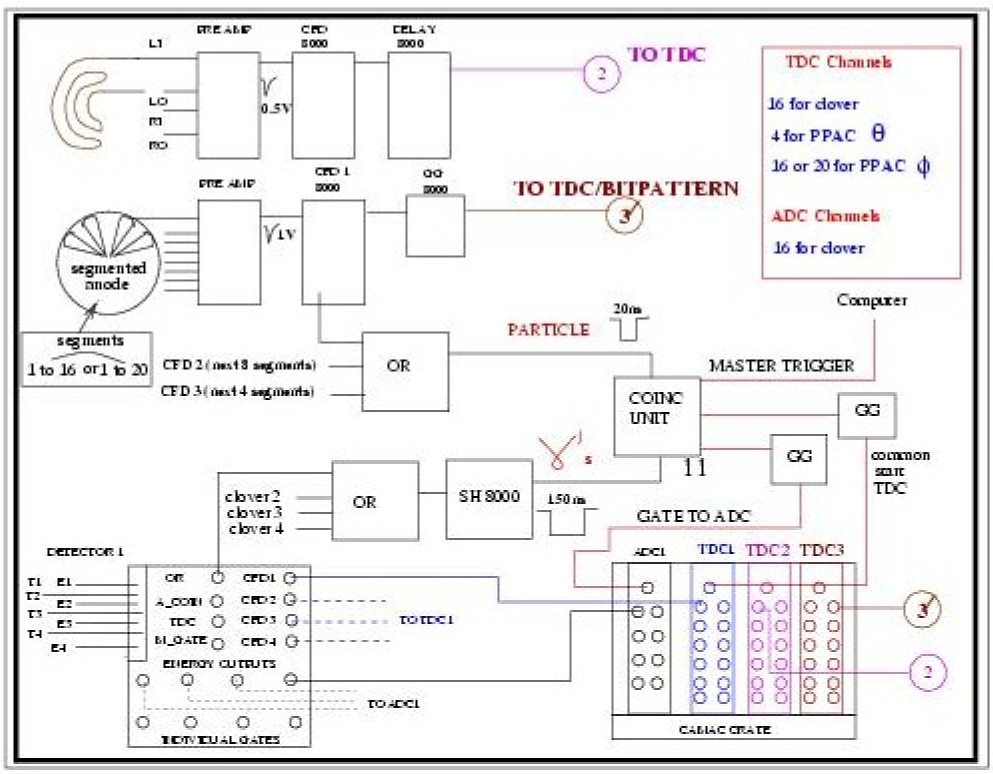

Fig. 4 shows the electronic block diagram of the particle-γ coincidence measurement.

We need the following electronic modules:

<u>PPAC:</u>

1. pre-amplifier (8-fold)
   3 modules for segmented anode (GSI)

1 module for delay-line cathode (GSI)

2. CFD-8000
   3 modules for segmented anode (GSI, fraction: 0.2, internal delay: 6ns)
   1 module for delay-line cathode (GSI, fraction: 0.4, internal delay:18ns)
3. GG-8000
   3 modules for segmented anode (GSI?)
4. 1 OR unit
5. DL-8000
   1 module for delay-line cathode

INGA clover:

1. clover module
   4 modules
2. 1 OR unit
3. 1 SH 8000

trigger:

1. 1 coincidence unit
2. 1 GG-8000 unit

ADC-TDC-BITPattern:

1. 1 16-channel ADC (Ge-detector)
2. 3 16-channel TDC (PPAC, Ge-detector)
3. 2 16-channel bit-pattern unit (if available)

4. On-line analysis

For controlling the experiment we need **raw spectra** for all parameters.

16 energy spectra (Ge-crystals)
4 time spectra (Ge-crystals)
4 time spectra (PPAC: left-inner, left-outer, right-inner, right-outer) range 4K
16-20 time spectra (PPAC: segmented anode).

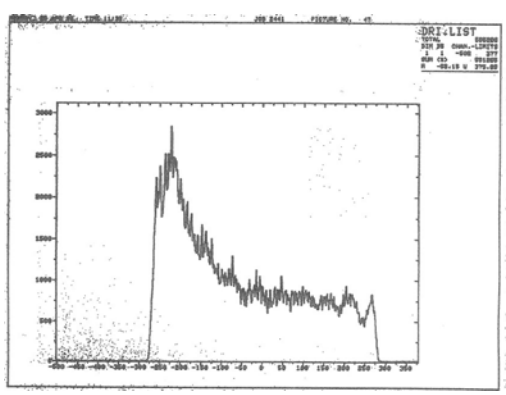

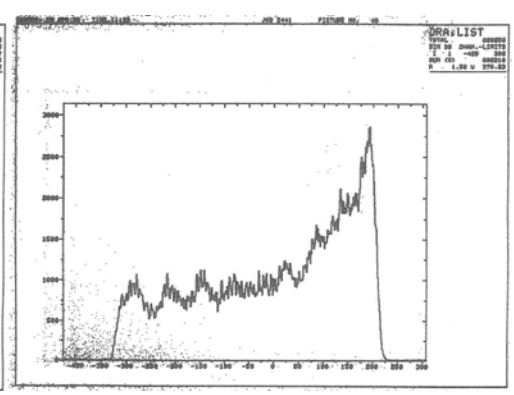

Fig. 5 shows delay-line spectra (delay right inner readout: t_{DRI}-t_R and delay right outer readout: t_{DRO}-t_R) for ^{206}Pb on ^{232}Th at 6.4MeV/u (CFD: fraction=0.4, delay=18ns).

2 difference spectra (PPAC delay line):

left-inner ─ left-outer   (range 8K)
right-inner ─ right outer (range 8K)

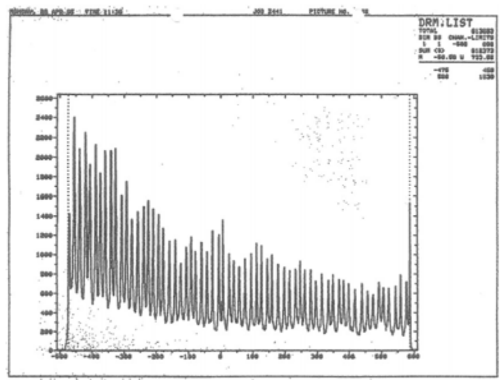

Fig. 6 shows difference spectrum (delay right inner readout - delay right outer readout: [t_{DRI}-t_R] – [t_{DRO}-t_R]) for ^{206}Pb on ^{232}Th at 6.4MeV/u (CFD: fraction=0.4, delay=18ns).

Some **spectra** have to be **calibrated**:

16 energy spectra in keV (Ge-crystals)
or 4 energy spectra in keV (INGA clover) to save computer storage
2 difference spectra (PPAC delay line) $\tan\vartheta = \frac{\tan 45^0 - \tan 15^0}{ch_2 - ch_1} \cdot (ch - ch_1) + \tan 15^0$

We need **look-up tables** for the segmented anodes and the INGA clover positions:

segment	IUAC	GSI
p1	22.5^0	18^0
p2	45.0^0	36^0
...	...	...
...	...	...
p16	360^0	288^0
p20		360^0

clover-1	30^0	0^0
clover-2	30^0	180^0
clover-3	150^0	0^0
clover-4	150^0	180^0

All angles should be stored in radian ($radian = \frac{\vartheta(\deg ree)\cdot\pi}{180^0}$ **).**

4.1 Doppler-shift correction

We have to perform **4 different Doppler shift corrections** (see appendix A), since we cannot identify the projectile ($15^0 \le \vartheta_3 \le 45^0$, $22.7^0 \le \theta_{cm} \le 66.5^0$) or recoil nucleus ($15^0 \le \vartheta_4 \le 45^0$, $150^0 \ge \theta_{cm} \ge 90^0$) with the PPAC. We also don't know if the projectile or recoil nucleus is excited.

The scattering angle is measured using the delay-line information (inner-outer difference)

$$\tan\vartheta = \frac{\tan 45^0 - \tan 15^0}{ch_2 - ch_1}\cdot(ch - ch_1) + \tan 15^0$$

From the PPAC anode segment we get the azimuthal angle φ (look-up table). The γ-ray direction is determined from the Ge-position $\vartheta_\gamma, \varphi_\gamma$ (look-up table).

64 Doppler corrected energy spectra in keV (Ge-crystals)
or
16 Doppler corrected energy spectra in keV (INGA clover) to save computer storage

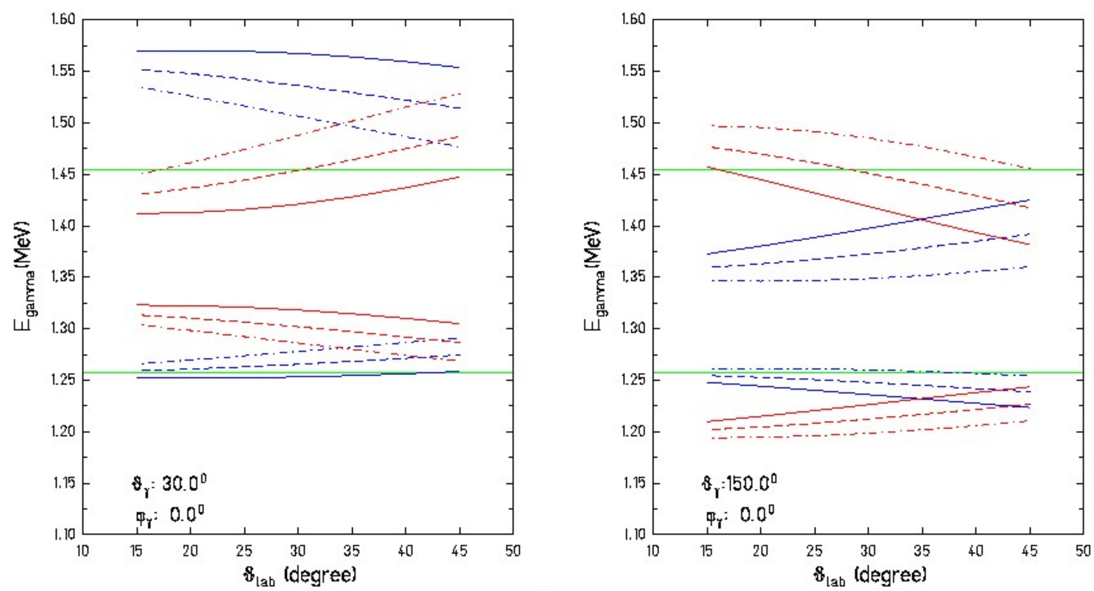

Fig.7 shows the Doppler shifted γ-ray energies for the ^{112}Sn excitation (2^+ energy: 1.257MeV) and ^{58}Ni excitation (2^+ energy: 1.454MeV) as a function of the laboratory scattering angle $\vartheta_{\ell ab}$. The γ-rays are measured at forward angles ($\vartheta_\gamma = 30^0$, $\varphi_\gamma = 0^0$, see left figure) and backward angles ($\vartheta_\gamma = 150^0$, $\varphi_\gamma = 0^0$, see right figure). The blue lines represent the results for distant collisions ($22.7^0 \le \theta_{cm} \le 66.5^0$, projectile detected), while the red lines are for close collisions ($150^0 \ge \theta_{cm} \ge 90^0$, target nucleus detected). The solid, dashed, dashed-dotted and dotted lines were calculated for azimuthal angles of $\varphi=0^0$, 90^0, 180^0 and 270^0, respectively. As expected, the dashed lines and the dotted lines coincide for the present calculations.

Calculations are performed with FORTRAN program: *doppler.f* *(www-linux.gsi.de/~wolle/INDIA)*

In the raw spectra the target excitation and the projectile excitation are clearly separated. After the Doppler shift correction the calculated γ-ray energy in the rest-frame should coincide with the green lines. The wrong corrected events contribute to the γ-ray background.

5. Coulomb excitation

5.1 'Safe' bombarding energy

The most straightforward way to the understanding of scattering of two heavy nuclei is obtained in the semiclassical approach. For large values of the Sommerfeld parameter η and large values of the wave number k_∞ the motion of the centers of the colliding nuclei can be described by classical orbits. Both parameters are defined by

Sommerfeld parameter: $\eta = 0.15746 \cdot Z_1 \cdot Z_2 \cdot \sqrt{\frac{A_1}{E_{\ell ab}}}$ *with* $E_{\ell ab}[MeV]$ *and* $A_i[amu]$

wave number: $k_\infty = 0.21872 \cdot \frac{A_1 \cdot A_2}{A_1 + A_2} \cdot \sqrt{\frac{E_{\ell ab}}{A_1}}$ *with* $E_{\ell ab}[MeV]$ *and* $A_i[amu]$

In our heavy ion reaction ^{58}Ni on ^{112}Sn at 175MeV both conditions (η=127 and $k_\infty=14.5fm^{-1}$) for a classical trajectory are fulfilled.

The experimental data can be displayed in dependence of the impact parameter, the angular momentum, the distance of closest approach and the scattering angle. In the distance of closest approach presentation, effects due to the nuclear interaction become nearly independent of dynamical quantities such as the bombarding energy. From these data one can obtain an estimate for the smallest distance of closest approach D_s for which the interaction between the two nuclei can be assumed to be purely electromagnetic. This distance can be used to calculate the maximum 'safe' bombarding energy, via the following formula $D = \frac{\eta}{k_\infty} \cdot \left[\sin^{-1}\left(\frac{\theta_{cm}}{2}\right) + 1\right] = 0.72 \cdot \frac{Z_1 \cdot Z_2}{E_{\ell ab}} \cdot \frac{A_1 + A_2}{A_2} \cdot \left[\sin^{-1}\left(\frac{\theta_{cm}}{2}\right) + 1\right]$.

Based on many experiments the smallest distance of closest approach D_s is well described by

$$D_s = C_1 + C_2 + 5\,fm$$

A minimum distance between the two nuclear surfaces of at least 5fm is needed to assure pure electromagnetic interaction. The matter half-density radii C_i have been calculated in the droplet model (W.D. Myers, Nucl.Phys.A204 (1973),465) by

$$C_i = R_i \cdot \left[1 - (1/R_i)^2\right]$$

with

$$R_i = 1.28 \cdot A_i^{1/3} - 0.76 + 0.8 \cdot A_i^{-1/3}$$

For ^{58}Ni (R_1=4.40fm, C_1=4.17fm) **on ^{112}Sn** (R_2=5.58fm, C_2=5.40fm) **experiment** the smallest distance of closest approach is D_s=14.57fm, from which **a maximum 'safe' bombarding energy of 210MeV can be calculated.**

5.1 Coulomb excitation cross section

Coulomb excitation calculations are performed with FORTRAN program: *lell30e1.f*
input-file: input, output-file: output and anggro.
Cross sections are integrated with FORTRAN program: *anggro.f*
input-file: input and coulex(=anggro see above), output-file: output
(www-linux.gsi.de/~wolle/INDIA)

In a first step the Coulomb excitation cross section (lell30e1.f) is calculated. Then we can distinguish 3 cases for the particle-γ angular correlation (anggro.f): **(i)** calculation in the rest-frame (I24=1, Q_0=1, Q_2=0, Q_4=0), **(ii)** calculation in the laboratory frame (only Lorentz-boost: I24=0, Q_0=1, Q_2=0, Q_4=0), **(iii)** calculation in the laboratory frame with γ-ray angular correlation (I24=0, Q_0=Q_2=Q_4=1). The results from anggro.f have to be multiplied by 4π to obtain the cross sections in [barn].

$\theta_\gamma\ \varphi_\gamma$	θ_{cm}		**^{112}Sn**: σ_2[mb] ^{58}Ni→^{112}Sn 175MeV	**^{58}Ni**: σ_2[mb] ^{58}Ni→^{112}Sn 175MeV	ratio ^{112}Sn/^{58}Ni
$30^0,0^0$	22.7^0-66.5^0	**(i)**	74.85	37.96	1.972
		(ii)	76.18	42.04	1.812
		(iii)	83.93	46.97	1.787
	150^0-90^0	**(i)**	82.98	48.22	1.721
		(ii)	88.56	48.78	1.816
		(iii)	109.66	61.61	1.780
150^0, 0^0	22.7^0-66.5^0	**(i)**	74.85	37.26	1.972
		(ii)	73.51	34.16	2.152
		(iii)	81.71	38.37	2.130
	150^0-90^0	**(i)**	82.98	48.22	1.721
		(ii)	77.65	47.55	1.633
		(iii)	97.74	59.00	1.657

How to determine the B(E2)-value:

$$B\left(E2;0^+ \rightarrow 2^+\right)\left[{}^{112}Sn\right] = B\left(E2;0^+ \rightarrow 2^+\right)\left[{}^{116}Sn\right] \cdot \frac{I_\gamma\left[{}^{112}Sn\right] / I_\gamma\left[{}^{58}Ni\right]}{I_\gamma\left[{}^{116}Sn\right] / I_\gamma\left[{}^{58}Ni\right]}$$

Proof of the equation:

$\theta_\gamma\ \varphi_\gamma$	θ_{cm}		**^{112}Sn**: σ_2[mb] ^{58}Ni→^{112}Sn 175MeV <2//M(E2)//0>=0.490eb	**^{112}Sn**: σ_2[mb] ^{58}Ni→^{112}Sn 175MeV <2//M(E2)//0>=0.539eb	ratio
$150^0,0^0$	22.7^0-66.5^0	**(iii)**	81.71	98.63	1.207

	150^0-90^0	**(iii)**	97.74	116.19	1.189

θ_γ φ_γ	θ_{cm}		**^{116}Sn**: σ_2[mb] ^{58}Ni→^{116}Sn 175MeV	**^{58}Ni**: σ_2[mb] ^{58}Ni→^{116}Sn 175MeV	ratio ^{116}Sn/^{58}Ni	double ratio ^{112}Sn/^{116}Sn
$30^0,0^0$	22.4^0-65.7^0	**(i)**	60.75	39.79	1.527	**1.292**
		(ii)	61.79	44.08	1.402	**1.293**
		(iii)	68.16	49.24	1.384	**1.291**
	150^0-90^0	**(i)**	70.74	51.24	1.381	**1.247**
		(ii)	75.39	51.76	1.457	**1.247**
		(iii)	93.38	65.37	1.429	**1.246**
150^0, 0^0	22.4^0-65.7^0	**(i)**	60.75	39.79	1.527	**1.316**
		(ii)	59.70	35.79	1.668	**1.290**
		(iii)	66.41	40.17	1.653	**1.288**
	150^0-90^0	**(i)**	70.74	51.24	1.381	**1.247**
		(ii)	66.30	50.60	1.310	**1.246**
		(iii)	83.45	62.77	1.330	**1.246**

θ_γ φ_γ	θ_{cm}		**^{120}Sn**: σ_2[mb] ^{58}Ni→^{120}Sn 175MeV	**^{58}Ni**: σ_2[mb] ^{58}Ni→^{120}Sn 175MeV	ratio ^{120}Sn/^{58}Ni	double ratio ^{112}Sn/^{120}Sn
$30^0,0^0$	22.2^0-65.0^0	**(i)**	86.46	41.46	2.085	**0.9455**
		(ii)	87.84	45.94	1.912	**0.9477**
		(iii)	95.97	51.26	1.872	**0.9544**
	150^0-90^0	**(i)**	94.53	54.17	1.745	**0.9861**
		(ii)	100.61	54.64	1.841	**0.9860**
		(iii)	124.50	69.03	1.804	**0.9869**
150^0, 0^0	22.2^0-65.0^0	**(i)**	86.46	41.46	2.085	**0.9633**
		(ii)	85.05	37.28	2.281	**0.9433**
		(iii)	93.70	41.80	2.242	**0.9500**
	150^0-90^0	**(i)**	94.53	54.17	1.745	**0.9861**
		(ii)	88.72	53.57	1.656	**0.9860**
		(iii)	111.61	66.45	1.680	**0.9863**

Coulomb excitation calculations are performed with FORTRAN program: *lell30e1.f*
input-file: input, output-file: output and anggro.
Cross sections [barns] are integrated with FORTRAN program: *angint.f*
input-file: INPUTang and coulex (see above), output-file: OUTPUT
(www-linux.gsi.de/~wolle/INDIA)

θ_{lab}	θ_{cm}	**^{112}Sn**: σ_2[mb] ^{58}Ni→^{112}Sn 175MeV	**^{58}Ni**: σ_2[mb] ^{58}Ni→^{112}Sn 175MeV	ratio ^{112}Sn/^{58}Ni
15^0-20^0	22.7^0-30.2^0	3.36	1.23	2.732
20^0-25^0	30.2^0-37.6^0	7.53	3.32	2.268
25^0-30^0	37.6^0-45.0^0	11.95	5.82	2.053
30^0-35^0	45.0^0-52.3^0	15.30	7.95	1.925
35^0-40^0	52.3^0-59.4^0	17.13	9.32	1.838
40^0-45^0	59.4^0-66.5^0	18.28	10.24	1.785
15^0-45^0	**22.7^0-66.5^0**	**73.56**	**37.88**	**1.942**
15^0-20^0	150^0-140^0	6.82	3.87	1.762
20^0-25^0	140^0-130^0	9.28	5.32	1.744
25^0-30^0	130^0-120^0	12.04	6.96	1.730
30^0-35^0	120^0-110^0	15.05	8.78	1.714
35^0-40^0	110^0-100^0	18.21	10.68	1.705
40^0-45^0	100^0-90^0	21.31	12.50	1.705
15^0-45^0	**150^0-90^0**	**82.70**	**48.11**	**1.719**

θ_{lab}	θ_{cm}	^{116}Sn: σ_2[mb] $^{58}Ni\rightarrow^{116}Sn$ 175MeV	^{58}Ni: σ_2[mb] $^{58}Ni\rightarrow^{116}Sn$ 175MeV	ratio $^{116}Sn/^{58}Ni$	double ratio $^{112}Sn/^{116}Sn$
15^0-20^0	22.4^0-29.8^0	2.50	1.29	1.938	1.410
20^0-25^0	29.8^0-37.2^0	5.97	3.50	1.706	1.329
25^0-30^0	37.2^0-44.5^0	9.56	6.08	1.572	1.306
30^0-35^0	44.5^0-51.7^0	12.43	8.34	1.490	1.292
35^0-40^0	51.7^0-58.7^0	14.07	9.76	1.442	1.275
40^0-45^0	58.7^0-65.7^0	15.14	10.75	1.408	1.268
15^0-45^0	**22.4^0-65.7^0**	**59.67**	**39.71**	**1.503**	**1.292**
15^0-20^0	150^0-140^0	5.81	4.11	1.414	1.246
20^0-25^0	140^0-130^0	7.92	5.65	1.402	1.244
25^0-30^0	130^0-120^0	10.27	7.40	1.388	1.246
30^0-35^0	120^0-110^0	12.84	9.33	1.376	1.246
35^0-40^0	110^0-100^0	15.52	11.35	1.367	1.247
40^0-45^0	100^0-90^0	18.13	13.30	1.363	1.251
15^0-45^0	**150^0-90^0**	**70.50**	**51.13**	**1.379**	**1.247**

θ_{lab}	θ_{cm}	^{120}Sn: σ_2[mb] $^{58}Ni\rightarrow^{120}Sn$ 175MeV	^{58}Ni: σ_2[mb] $^{58}Ni\rightarrow^{120}Sn$ 175MeV	ratio $^{120}Sn/^{58}Ni$	double ratio $^{112}Sn/^{120}Sn$
15^0-20^0	22.2^0-29.5^0	4.36	1.35	3.230	0.846
20^0-25^0	29.5^0-36.8^0	9.36	3.62	2.586	0.877
25^0-30^0	36.8^0-44.0^0	13.99	6.29	2.224	0.923
30^0-35^0	44.0^0-51.1^0	17.44	8.63	2.021	0.953
35^0-40^0	51.1^0-58.1^0	19.50	10.29	1.895	0.970
40^0-45^0	58.1^0-65.0^0	20.37	11.21	1.817	0.982
15^0-45^0	**22.2^0-65.0^0**	**85.02**	**41.38**	**2.055**	**0.945**
15^0-20^0	150^0-140^0	7.93	4.35	1.823	0.967
20^0-25^0	140^0-130^0	10.71	5.98	1.791	0.974
25^0-30^0	130^0-120^0	13.79	7.83	1.761	0.982
30^0-35^0	120^0-110^0	17.14	9.87	1.737	0.987
35^0-40^0	110^0-100^0	20.63	11.99	1.721	0.991
40^0-45^0	100^0-90^0	24.06	14.06	1.711	0.997
15^0-45^0	**150^0-90^0**	**94.27**	**54.07**	**1.744**	**0.986**

expected beam current: $0.5\,pnA \equiv 3.125\cdot 10^{9}\ ions/s$

target thickness: $0.5\ mg/cm^2 \equiv 2.69\cdot 10^{18}\ nuclei/cm^2$

event rate [s^{-1}] = luminosity * cross section = $8.40\cdot 10^{27}\cdot cross\ section\left[cm^2\right]$

For a cross section of 100mb, an intrinsic photopeak efficiency ε=0.13 and a solid angle of Ω=0.0183 (r=3.25cm, R=12cm) one obtains an **event rate of 2[s^{-1}]**.

Appendix A: Doppler shift correction

1.case: ^{58}Ni measured with PPAC, ^{58}Ni excited

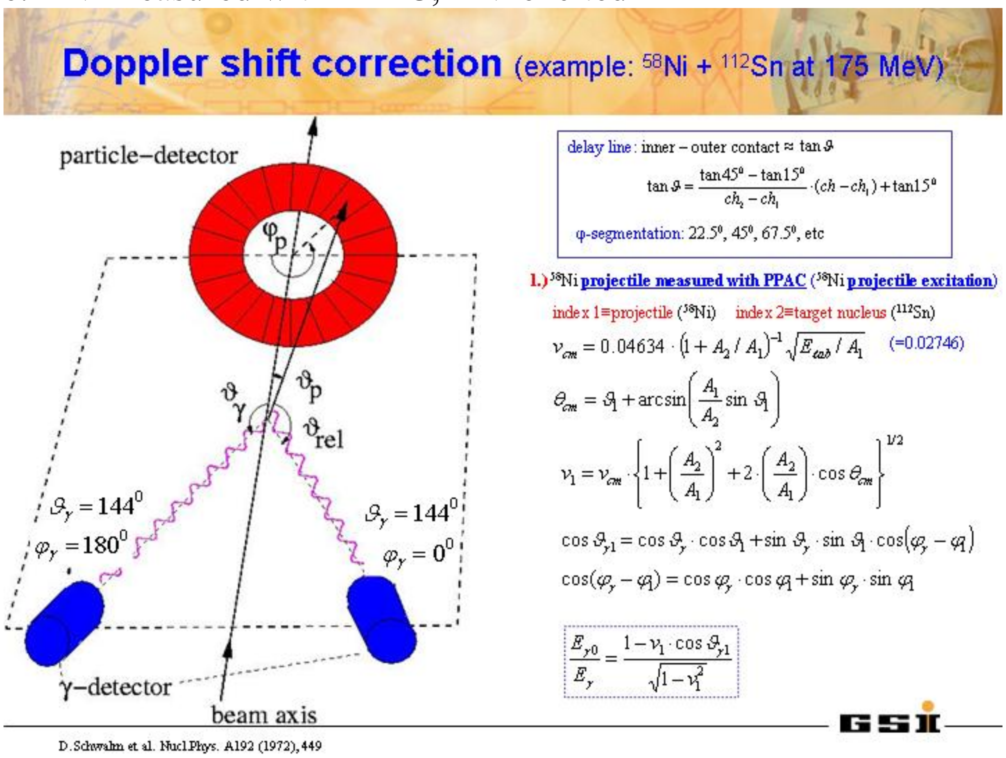

2.case: ^{58}Ni measured with PPAC, ^{112}Sn excited

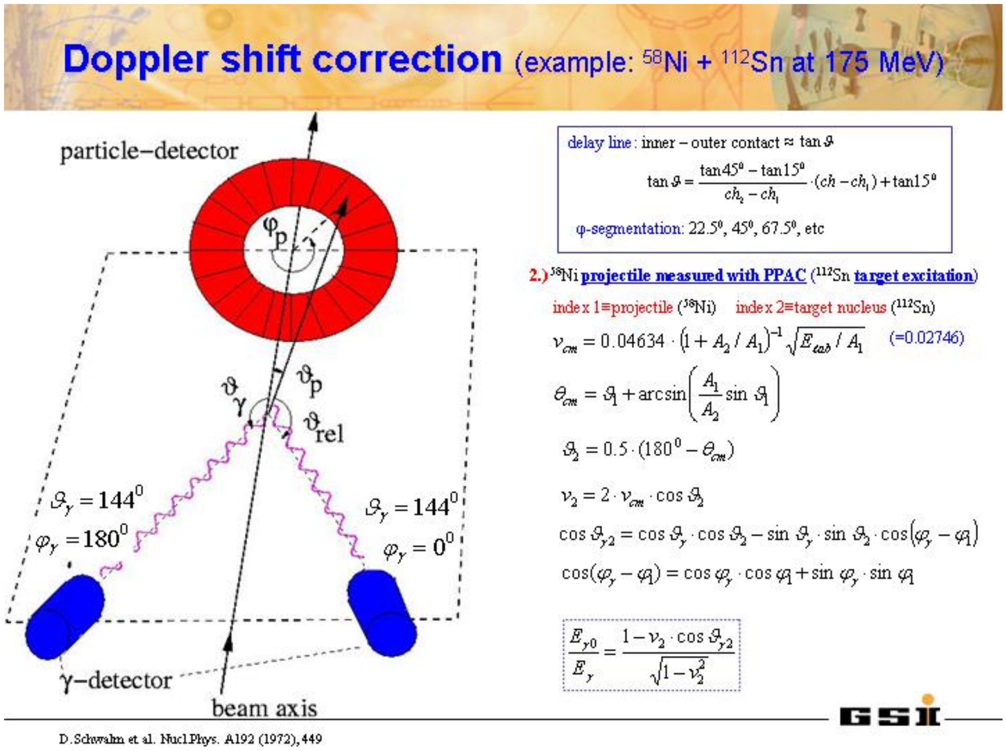

3.case: ^{112}Sn measured with PPAC, ^{112}Sn excited

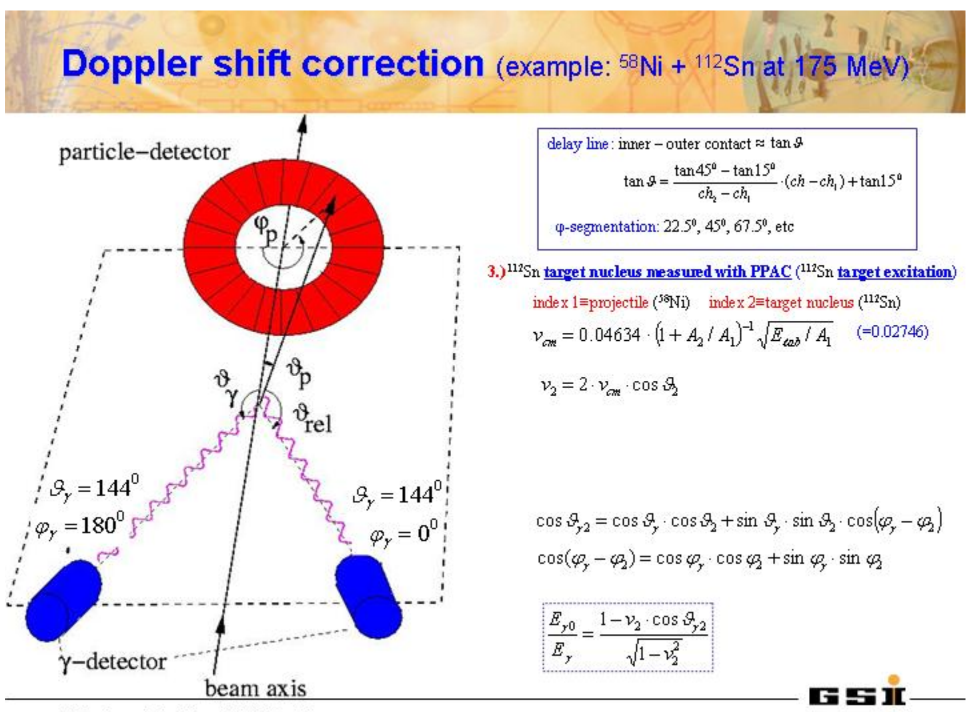

4.case: ^{112}Sn measured with PPAC, ^{58}Ni excited

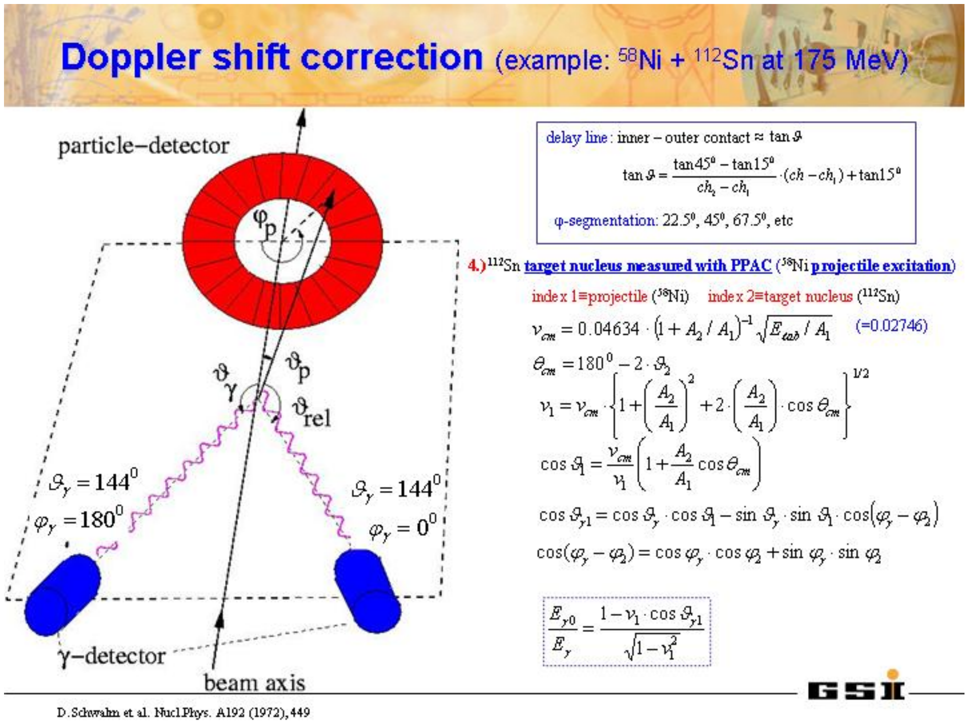

Appendix B: Analysis of Target Material

4/119996/97

TRACE SCIENCES INTERNATIONAL

CERTIFICATE OF ANALYSIS

#1

Name of Preparation: ^{112}Sn

Country of Destination: Germany

Consignee: GSI

CHARACTERISTICS OF ISOTOPE-ENRICHED PRODUCT

1. Weight of enriched isotope:

Compound weight: 5,000 mg. **Element weight: 5,000 mg.**

Form: Sn (Metal Foil)

2. Isotopic composition:

Isotope	112	114	115	116	117	118	119	120
Enrichment (%)	**99.5+/- 0.2**	0.2+/- 0.1	<0.1	<0.1	<0.1	0.3+/- 0.1	<0.05	<0.05
Isotpe	122	124						
Enrichment (%)	<0.05	<0.05						

3. Chemical Impurities:

Cmpds of	Ca	Si	Fe	Cu	Ag	Al	Mg	Mn
P.P.M.	100	50	60	5	4	1	80	15
Cmpds of	Pb	Sb	Ni	Cr				
P.P.M.	25	<50	<50	<50				

4. Analytical method: ICP-MS

Signature

(PLEASE NOTE THIS MATERIAL IS NOT APPROVED FOR USE IN HUMANS)

15 WERTHEIM COURT, SUITE 404, RICHMOND HILL, ONTARIO, CANADA L4B 3H7 Telephone: (905) 707-7000 Fax: (905) 707-0700

98.00% w.t. 116 50 Sn

3/27901/90

11. JUNI 1990

EXPORT

QUALITY CERTIFICATE No 89-4.a

Name of preparation - TIN-118
Supplier v/o "Techsnabexport" Order No 1860348/02-142-0175
Country of distination FRG

CHARACTERISTICS OF ISOTOPE - ENRICHED PRODUCT

1. Weight of enriched isotopic mixture Sn
Compound weight 5000 ,mg, element weight 5000 mg.
2. Isotopic content:

Isotope	112	114	115	116	117	118
Percentage (%%)	< 0.0200	< 0.0100	0.0400	98.0000 +-0.100	0.6800	0.7000

Isotop	119	120	122	124		
Percentage (%%)	0.0900	0.3100	0.0400	0.1400		

3. Chemical admixtures:

Elements	Fe	Al	Si	Cr	Ni	Cu	Pb
Percentage (%%)	0.00800	0.00300	0.00500	< 0.00300	0.00500	0.00400	< 0.00200
Elements	Sb	Bi	Zn	As			
Percentage (%%)	< 0.00300	< 0.00200	0.02400	< 0.00020			

Measurement data of above-mentioned preparation comply with technical, specifications now in force USSR and with order requirements.

Signature

H. Emling

7/97042/87

EXPORT 4.383

MEASUREMENT CERTIFICATE
СЕРТИФИКАТ О КАЧЕСТВЕ

91

issued 9. 02 19 83
Выдан

Name of preparation / Наименование препарата: TIN - 120

Contractor / Заказчик:

Order No / Заказ-наряд: 54/02-117-3164

Country of destination / Страна назначения: B R D

Consignee / Получатель:

Marking / Маркировка:

CHARACTERISTICS OF ISOTOPE — ENRICHED PRODUCT
ХАРАКТЕРИСТИКА ИЗОТОПИЧЕСКИ ОБОГАЩЕННОГО ПРОДУКТА

1. Weight of enriched isotopic mixture / Вес обогащенной изотопной смеси: Sn

Compound weight / Лигатурный ______ mg, МГ, element weight / элементарный 200 mg, МГ

2. Isotopic content
Изотопный состав

Isotope Изотоп	112	114	115	116	117	118	119	120	122	124
Percentage Содержание (%%)	<0,01	<0,01	<0,01	0,04	0,06	0,10	0,13	99,6 ±0,1	0,05	0,02

3. Chemical admixtures:
Химические примеси

Elements Элементы	Fe	Al	Si	Cr	Ni	Cu	Pb	Sb	Bi	Zn	As								
Percentage Содержание (%%)	0,006	0,005	0,007	<0,003	<0,004	0,006	<0,002	<0,003	<0,002	<0,003	<0,0002								

4. Remark:
Примечание:

Measurement data of above-mentioned preparation comply with technical, specifications now in force in USSR and with order requirements.

Указанный в настоящем сертификате препарат соответствует по качеству действующим в СССР техническим условиям и требованиям заказ-наряда.

Signature / Подпись

Appendix C: Nuclear Structure Data

isotope	I^π energy(MeV)	$I_i \rightarrow I_f$ B(E2;$I_i \rightarrow I_f$)	<I_f//M(E2)//I_i> eb	τ (ps)
^{112}Sn	2_1^+ 1.257	$0_1^+ \rightarrow 2_1^+$ 0.240(14)	0.490(14)	0.542(52)
	2_2^+ 2.151	$0_1^+ \rightarrow 2_2^+$ 0.0007(2)	0.026(4)	
		$2_1^+ \rightarrow 2_2^+$ 0.037(15)	0.430(80)	
	0_2^+ 2.191			
	4_1^+ 2.355	$2_1^+ \rightarrow 4_1^+$ 0.032(5)	0.403(32)	
^{116}Sn	2_1^+ 1.294	$0_1^+ \rightarrow 2_1^+$ 0.209(6)	0.457(7)	0.538(15)
	2_2^+ 2.112	$0_1^+ \rightarrow 2_2^+$ 0.0011(4)	0.032(6)	
		$2_1^+ \rightarrow 2_2^+$ 0.013(5)	0.255(45)	
	4_1^+ 2.391	$2_1^+ \rightarrow 4_1^+$ 0.137(25)	0.827(73)	
		$2_2^+ \rightarrow 4_1^+$ 0.360(72)	1.342(128)	
^{120}Sn	2_1^+ 1.171	$0_1^+ \rightarrow 2_1^+$ 0.202(4)	0.449(4)	0.918(18)
^{58}Ni	2_1^+ 1.454	$0_1^+ \rightarrow 2_1^+$ 0.0705(18)	0.266(3)	0.891(22)
		$0_1^+ \rightarrow 2_1^+$ 0.0493(18)	0.222(4)	
	4_1^+ 2.459	$2_1^+ \rightarrow 4_1^+$ 0.0264(24)	0.363(17)	

lifetime of the 2^+ state:

$$\tau[s] = \left\{ \left[1 + \alpha_T(E2)\right] \cdot 1.225 \cdot 10^{13} \cdot E_\gamma[MeV]^5 \cdot B(E2;2^+ \rightarrow 0^+)\left[e^2 b^2\right] \right\}^{-1}$$

relation between B(E2)-values:

$$B\left(E2;2^+ \rightarrow 0^+\right) = \frac{1}{5} \cdot B(E2;0^+ \rightarrow 2^+)$$

reduced matrix elements:

$$B\left(E2;0^+ \rightarrow 2^+\right) = \left\langle 2^+ \| M(E2) \| 0^+ \right\rangle^2$$

Appendix D: Input Data for Coulomb Excitation-Program lell30e1.f

data card #	parameter	input describtion
1	NMAX	number of nuclear states
2	NCM	index of level for which the lab-transformation is done
3	NTIME	-
4	XIMAX	largest number for ξ-parameter
5	EMMAX1	largest magnetic quantum number considered
6	ACCUR	absolute accuracy to which the final probabilities should be computed
	QPAR	effect of the giant dipole resonance
7	OUXI	print-out of ξ-matrix
8	OUPSI	print-out of ψ-matrix
9	OUAMP	print-out of excitation amplitudes
10	OUPROW	print-out of excitation probability during integration
11	OUANG0	print-out of angular distribution coefficients α^0
12	OUANG1	print-out of angular distribution coefficients α^1
13	OUANG2	print-out of angular distribution coefficients α^2
14	OUANG3	print-out of angular distribution coefficients α^3
15	NCORR	-
16	INTERV	number of integration steps
17	Z1	charge number of the projectile
	A1	mass of projectile [amu]
18	Z2	charge number of the target nucleus
	A2	mass of target nucleus [amu]
19	EP	laboratory energy of projectile [MeV]
20	TLBDG	deflection angle [degree] in the lab-system
21	THETA	deflection angle [degree] in the cm-system
22	N	index of level
	SPIN(N)	spin quantum number of the Nth nuclear state
	EN(N)	excitation energy of the Nth nuclear state
	IPAR(N)	parity (-1 neg, 1 pos) of the Nth nuclear state
23	N	index of level
	M	index of level (M≥N)
	ME(N,M,LA)	electric matrix element
	LA	multipolarity (1≤LA≤6)
0		starts the calculation
500		stops the calculation

Appendix E: Input Data for Angular Distribution-Program anggro.f

data card #	parameter	input describtion
1	I11	output of the conversion coefficients (E2,M1,E1,E3)
	I12	possible decays of a state
	I13	HN (lifetime of the state)
	I14	G_K(N,M)
	I15	F_K(N,M)
	I16	$\alpha^3(k,\kappa)$+feeding
	I17	Spin(N),Spin(M),W(N,K)
	I18	Spin(N),Spin(M),DS(N,K)
	I19	γ-ray angular distribution $\theta_\gamma=0^0,180^0,5^0$ $\varphi_\gamma=0^0$ and 180^0
	I20	-
	I21	excitation probabilities, cross sections, $\alpha^3(k,\kappa)$
	I22	1≡solid angle correction, 2≡ +deorientation, 3≡ +SB
	I23	input M1-matrix element + M1 conversion coefficient
	I24	1≡calc. in rest system, >1 input of θ_γ, φ_γ in rest system
	I25	projectile excitation
2	NCCK	number of values given for K-conversion
	NCCL	number of values given for L-conversion
	NCCM	number of values given for M-conversion
3-5	CCE1	lowest tabulated energy to be interpolated, -1.0 for L,M
	CCE2	lowest tabulated energy of the K, L2, M5 subshell
	CCMIN	min. energy given in the conversion table
	CCMAX	max. energy given in the conversion table
6_1-	α_K,I=1,NCCK	conversion coefficients (K-shell)
7_1-	α_L,I=1,NCCL	conversion coefficients (L-shell)
8_1-	α_M,I=1,NCCM	conversion coefficients (M-shell)
9	IXYZ	I23=1 IXYZ=initial state
	JXYZ	I23=1 JXYZ=final state
	MM1(IXYZ,JXYZ))	I23=1 M1-matrix element (IXYZ→JXYZ)
10	TT	θ_γ
	VGAMMA	φ_γ
	VI1	φ_1
	VI2	φ_γ
	K1LAB	state for cm to lab transformation
11	Q_0,Q_2,Q_4	I22=1 solid angle correction for Ge-detector
		I22=2, I22=3, I22=4, I22=5 (see program)
12	MZahl	number of theta integrations
	NORM	normalization, neg. value ≡ Rutherford
13	XA	initial scattering angle in cm system for integration
	XE	final scattering angle in cm system for integration

Appendix F: Important Formulas

nuclear lifetime:

$$\tau[s] = \left\{ \sum_M \sum_L \delta^2_{N\to M}(L) \cdot [1 + \alpha_{N\to M}(L)] \right\}^{-1}$$

with

$$\delta^2_{N\to M}(E2)\left[s^{-1}\right] = 1.225 \cdot 10^{13} \cdot E_\gamma[MeV]^5 \cdot B(E2; I_N \to I_M)\left[e^2 b^2\right]$$

$$\delta^2_{N\to M}(M1)\left[s^{-1}\right] = 1.758 \cdot 10^{13} \cdot E_\gamma[MeV]^3 \cdot B(M1; I_N \to I_M)\left[\frac{e\hbar}{2m_p c}\right]^2$$

$$\delta^2_{N\to M}(E1)\left[s^{-1}\right] = 1.590 \cdot 10^{17} \cdot E_\gamma[MeV]^3 \cdot B(E1; I_N \to I_M)[eb]$$

$$\delta^2_{N\to M}(E3)\left[s^{-1}\right] = 5.709 \cdot 10^{8} \cdot E_\gamma[MeV]^7 \cdot B(E3; I_N \to I_M)\left[e^3 b^3\right]$$

relation between B(E2) values:

$$B(EL; I_N \to I_M) = \frac{2 \cdot I_M + 1}{2 \cdot I_N + 1} \cdot B(EL; I_M \to I_N)$$

reduced matrix element

$$B(EL; I_M \to I_N) = \frac{1}{2 \cdot I_M + 1} \cdot \left\langle I_N \| M(EL) \| I_M \right\rangle^2$$

Coulomb excitation cross section (single state excitation):

$$\boldsymbol{\sigma_{E2}} = 4.918 \cdot (1 + A_1 / A_2)^{-2} \cdot \frac{A_1}{Z_2^2} \cdot (E_{MeV} - (1 + A_1 / A_2) \cdot \Delta E_{MeV}) \cdot \mathbf{B(E2; 0^+ \to 2^+)} \cdot f_{E2}(\xi)$$

with

$$\xi = \frac{Z_1 \cdot Z_2 \cdot A_1^{1/2} \cdot \Delta E'_{MeV}}{12.65 \cdot \left(E_{MeV} - 0.5 \cdot \Delta E'_{MeV}\right)^{3/2}} \quad with \quad \Delta E'_{MeV} = (1 + A_1 / A_2) \cdot \Delta E_{MeV}$$

Appendix G: Transformation of a polar coordinate system from target position to a flat (Ge) detector

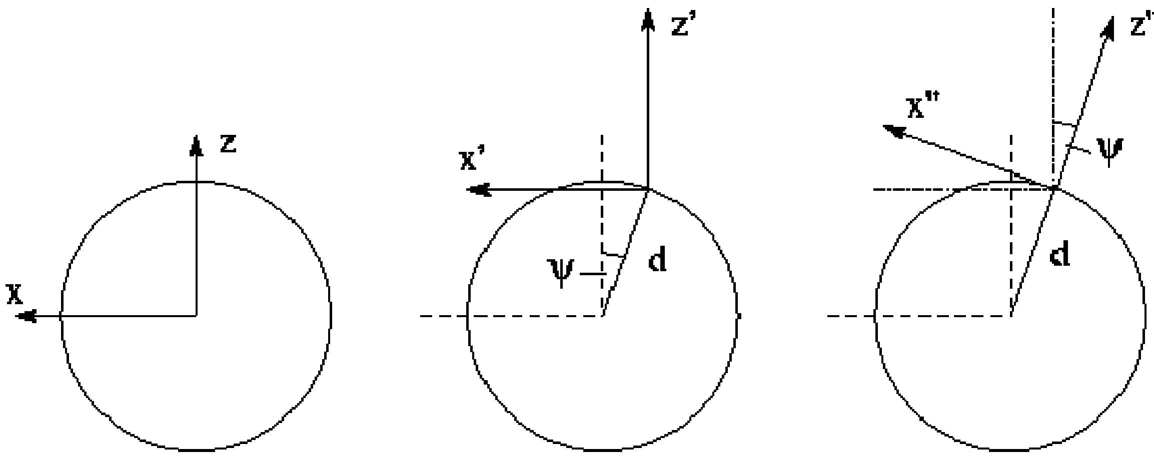

Figure: Left: polar coordinate system in target position (y-axis points out of plane); center: coordinate system moved in detector position (d=distance between detector and target, **ψ=-20^0**); right: coordinate system rotated around the y-axis (**ψ=-20^0**) to measure events from the target.

1.) Polar coordinate system with its origin in target position (y-axis points upwards)

$$x = r \cdot \sin\vartheta \cdot \cos\varphi$$
$$y = r \cdot \sin\vartheta \cdot \sin\varphi$$
$$z = r \cdot \cos\vartheta$$

2.) The origin of the coordinate system is shifted to the detector surface (d = distance from detector surface to target position, ψ-angle is negative for the displayed example in figure)

$$x' = x - d \cdot \sin\psi$$
$$y' = y$$
$$z' = z - d \cdot \cos\psi$$

3.) The coordinate system is rotated around y-axis (ψ-angle is negative for the displayed example in figure)

$$x'' = x' \cdot \cos\psi - z' \cdot \sin\psi$$
$$y'' = y'$$
$$z'' = x' \cdot \sin\psi + z' \cdot \cos\psi$$

Boundary condition z''=0 for flat detector surface

$$
\begin{aligned}
z'' = 0 &= \left(x - d \cdot \sin\psi\right) \cdot \sin\psi + \left(z - d \cdot \cos\psi\right) \cdot \cos\psi \\
&= x \cdot \sin\psi + z \cdot \cos\psi - d \\
&= r \cdot \sin\vartheta \cdot \cos\varphi \cdot \sin\psi + r \cdot \cos\vartheta \cdot \cos\psi - d
\end{aligned}
$$

$$
r = \frac{d}{\cos\vartheta \cdot \cos\varphi + \sin\vartheta \cdot \sin\psi \cdot \cos\varphi}
$$

One obtains the following relation for a point (x'',y'') on the detector surface and the polar angle ϑ and the azimuthal angle φ:

$$
\frac{x''}{d} = \frac{\sin\vartheta \cdot \cos\varphi \cdot \cos\psi - \cos\vartheta \cdot \sin\psi}{\cos\vartheta \cdot \cos\psi + \sin\vartheta \cdot \sin\psi \cdot \cos\varphi}
$$

$$
\frac{y''}{d} = \frac{\sin\vartheta \cdot \sin\varphi}{\cos\vartheta \cdot \cos\psi + \sin\vartheta \cdot \sin\psi \cdot \cos\varphi}
$$

$$
\cos\vartheta = \frac{\cos\psi - \frac{x''}{d} \cdot \sin\psi}{\sqrt{\left(\frac{x''}{d}\right)^2 + \left(\frac{y''}{d}\right)^2 + 1}}
$$

$$
\cos\varphi = \frac{\frac{x''}{d} \cdot \cos\psi + \sin\psi}{\tan\vartheta \cdot \left[\cos\psi - \frac{x''}{d} \cdot \sin\psi\right]}
$$

Calculation of the clover crystal angles

The INGA-clover detector has 4 Ge-crystals which are displayed below

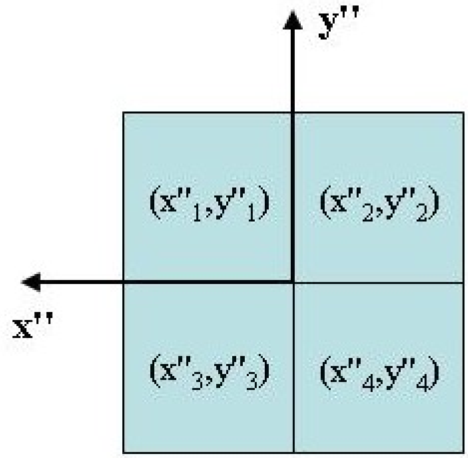

Polar- (ϑ) and azimuthal (φ) angles of the INGA-clover crystals for $\psi=153^0$, x''/d=y''/d=0.25 and d=12cm

x''/d	y''/d	ϑ ($\psi=-153^0$)	φ ($\psi=-153^0$)
0.25	0.25	137.14^0	20.29^0
0.25	-0.25	137.14^0	-20.29^0
-0.25	0.25	161.27^0	47.25^0
-0.25	-0.25	161.27^0	-47.25^0